European Journal of Neuroscience, Vol. 27, pp. 1801–1808, 2008 doi:10.1111/j.1460-9568.2008.06137.x

Drifting grating stimulation reveals particular activation properties of visual neurons in the caudate nucleus

Attila Nagy,[1] Zsuzsanna Paróczy,[1] Zita Márkus,[1] Antal Berényi,[1] Marek Wypych,[2] Wioletta J. Waleszczyk[2] and György Benedek[1]
[1]Department of Physiology, Faculty of Medicine, Albert Szent-Györgyi Medical and Pharmaceutical Center, University of Szeged, Dóm tér 10., H-6720 Szeged, Hungary
[2]Department of Neurophysiology, Nencki Institute of Experimental Biology, 3 Pasteur St., 02-093 Warsaw, Poland

Keywords: basal ganglia, cat, motion detection, spatial and temporal frequency tuning, temporal modulation

Abstract

The role of the caudate nucleus (CN) in motor control has been widely studied. Less attention has been paid to the dynamics of visual feedback in motor actions, which is a relevant function of the basal ganglia during the control of eye and body movements. We therefore set out to analyse the visual information processing of neurons in the feline CN. Extracellular single-unit recordings were performed in the CN, where the neuronal responses to drifting gratings of various spatial and temporal frequencies were recorded. The responses of the CN neurons were modulated by the temporal frequency of the grating. The CN units responded optimally to gratings of low spatial frequencies and exhibited low spatial resolution and fine spatial frequency tuning. By contrast, the CN neurons preferred high temporal frequencies, and exhibited high temporal resolution and fine temporal frequency tuning. The spatial and temporal visual properties of the CN neurons enable them to act as spatiotemporal filters. These properties are similar to those observed in certain feline extrageniculate visual structures, i.e. in the superior colliculus, the suprageniculate nucleus and the anterior ectosylvian cortex, but differ strongly from those of the primary visual cortex and the lateral geniculate nucleus. Accordingly, our results suggest a functional relationship of the CN to the extrageniculate tecto-thalamo-cortical system. This system of the mammalian brain may be involved in motion detection, especially in velocity analysis of moving objects, facilitating the detection of changes during the animal's movement.

Introduction

The caudate nucleus (CN) is the main structure receiving sensory–motor information incoming to the basal ganglia in the mammalian brain. It is involved in visuomotor behavior and contributes to the control of visually guided oculomotor and skeletomotor functions (Lynd-Balta & Haber, 1994; Barneoud *et al*., 2000; Hikosaka *et al*., 2000). Accordingly, a number of studies have been performed to clarify the role of the CN in visual information processing (Pouderoux & Freton, 1979; Rolls *et al*., 1983; Strecker *et al*., 1985; Hikosaka *et al*., 1989; Kolomiets, 1993; Brown *et al*., 1995; Nagy *et al*., 2003b). The CN neurons have been found to possess particular visual receptive field properties. Extracellular recordings in anesthetized cats revealed extremely large visual receptive fields that cover almost the whole of the approachable visual field of the eye, and consequently there is an absence of retinotopical organization (Pouderoux & Freton, 1979; Nagy *et al*., 2003b, 2005). These receptive field properties are in no way in accordance with those described in the neurons of the geniculostriate pathway. This supports the notion that the visual neuronal mechanisms of the basal ganglia represent particular dynamic properties differing from those of the primary visual cortex. Although visual information processing depends critically upon the integration of spatial and temporal information, no study has yet been performed concerning the responses of the CN neurons to sinewave drifting gratings. The sinusoidally modulated grating is an elementary component of the visual scene in the sense that any two-dimensional visual object can be represented by an appropriate combination of these gratings (De Valois *et al*., 1979; Pinter & Harris, 1981). Responses of neurons to drifting gratings of different spatial and temporal frequencies can be interpreted in terms of the dimensions and distribution of spatially and temporally summed excitatory and inhibitory components within their receptive fields (Enroth-Cugell & Robson, 1966; Zumbroich *et al*., 1988). Thus, a description of the hitherto unknown spatiotemporal filter properties of the CN neurons can contribute to an understanding of the role of the striatum in visual information processing and the connected behavioral sensorimotor actions.

Correspondence: Dr A. Nagy, as above.
E-mail: nagya@phys.szote.u-szeged.hu

Received 6 August 2007, revised 6 February 2008, accepted 7 February 2008

Materials and methods

Animal preparation and surgery

The experiments were carried out on six adult cats of either sex weighing from 2.5 to 4.0 kg. All procedures were carried out so as to minimize the number of animals used and followed the European Communities Council Directive of 24 November 1986 (S6609 EEC) and the National Institutes of Health Guidelines for the Care and Use of Animals for Experimental Procedures. The experimental protocol had been accepted by the Ethical Committee for Animal Research at Albert Szent-Györgyi Medical and Pharmaceutical Center at the University of Szeged.

The animals were initially anesthetized with ketamine hydrochloride (30 mg/kg, i.m., Calypsol). An s.c. injection of 0.2 mL 0.1% atropine sulfate was administered preoperatively to reduce salivation and

bronchial secretion. The trachea and the femoral vein were cannulated and the animals were placed in a stereotaxic head holder. All wound edges and pressure points were treated appropriately with procaine hydrochloride (1%). Anesthesia was maintained with halothane (1.6% during surgery and 0.8% during recordings). The depth of anesthesia was monitored by continuous reading of the end-tidal halothane values and by repeated checks of the electroencephalogram (EEG) and the electrocardiogram. There was continuous high-amplitude, low-frequency EEG activity, and we checked repeatedly whether interventions or forceful pressing of the forepaws induced desynchronization. The minimum alveolar anesthetic concentration values calculated from the end-tidal halothane readings always lay in the range given by Villeneuve & Casanova (2003). The animals were then immobilized with gallamine triethiodide (20 mg/kg i.v., Flaxedyl). During recording sessions, a liquid containing gallamine triethiodide (8 mg/kg/h), glucose (10 mg/kg/h) and dextran (50 mg/kg/h) in Ringer's lactate solution was infused at a rate of 3 mL/kg/h. End-tidal CO_2 level and rectal temperature were monitored continuously, and were maintained approximately constant, at 3.8–4.2% and 37–38 °C, respectively. The skull was opened to allow a vertical approach to the CN. The dura was removed and the cortical surface was covered with a 4% solution of agar dissolved in Ringer's solution. The eye contralateral to the recording was treated with phenylephrine (10%) and atropine (0.1%), and was equipped with a +2 diopter contact lens. The ipsilateral eye was covered during stimulation. The retinal landmarks and major retinal blood vessels were projected routinely twice daily onto a tangent screen, using a fiberoptic light source (Pettigrew *et al*., 1979). In some cases, the area centralis could be imaged directly; in others, it was plotted by reference to the optic disk, 14.6° medially and 6.5° below the center of the optic disk (Bishop *et al*., 1962).

Recording

Electrophysiological recordings of single units were carried out extracellularly via tungsten microelectrodes (AM System Inc., USA; 2–4 MΩ). Vertical penetrations were performed between the Horsley-Clarke coordinates anterior: 12–16, lateral: 4–6.5 in the stereotaxic depths 12–19, to record CN single-units. At the end of the experiments, the animals were deeply anesthetized with pentobarbital (200 mg/kg i.v.) and transcardially perfused with 4% paraformaldehyde solution. The brains were removed and cut into 50-μm coronal sections, and the sections were stained with Neutral Red. Recording sites were localized on the basis of the marks of the electrode penetrations. The recorded neurons were located in the dorsolateral aspect of the CN.

Visual stimulation and data analysis

For visual stimulation, an 18-inch computer monitor (refresh rate, 85 Hz) was placed 42.9 cm in front of the animal. The diameter of the stimulation screen was 22.5 cm, and the cat therefore saw it under 30° (if the stimulus diameter on a tangent screen is 22.5 cm and the distance between the eye and the centre point of the screen is 42.9 cm the viewing angle of the stimulus is 30 degrees). The mean luminance of the screen was 23 cd/m^2. For studies of the spatiotemporal characteristics of the cells, high-contrast (96%) drifting sinusoidal gratings were used. The sinusoidal gratings were moved along four different axes in eight different directions (0–315° at 45° increments) to find the optimal moving direction of each unit. The optimal direction of each unit was further used to describe its spatial and temporal characteristics. The tested spatial frequencies ranged from 0.025 to 0.4 cycles/° (c/°) and the temporal frequencies from 0.07 to 37.24 cycles/s (Hz). Stimuli were presented in a pseudo-random sequence in a series consisting of eight spatiotemporal frequency combinations of moving gratings. Each spatiotemporal frequency combination was presented at least 12 times. The interstimulus interval was consistently 1 s. Individual action potentials were distinguished with the help of a spike-separator system (SPS-8701; Australia). The number and temporal distribution of the action potentials recorded during stimulation were stored as peristimulus time histograms (PSTHs, 10-ms bin) and analysed off line. The duration of the prestimulus time (a stationary sinusoidal grating was shown) was 1000 ms, similar to the peristimulus time (a drifting sinusoidal grating was shown). The net discharge rate, calculated as the difference between the mean firing rates of the cell obtained during stimulus movement and the background activity corresponding to the mean activity during the 200 ms preceding movement in the prestimulus period, was used to characterize the response amplitude of the CN neurons. To estimate the extent of direction selectivity, a direction selectivity index (*DI*) similar to that proposed by Dreher *et al*. (1993) was calculated by using the formula:

$$DI = 100 \times (R_p - R_{np})/R_p$$

where R_p and R_{np} are the net discharge rates in the preferred and nonpreferred (opposite) directions, respectively.

A majority of the CN neurons exhibited a modulated response to the drifting gratings. The relative modulation index (*MI*) was calculated as the ratio of the amplitude of the response component at the fundamental (i.e. the stimulus) temporal frequency (f_1) and the net response of the cell (f_0) (Movshon *et al*., 1978a):

$$MI = f_1/f_0$$

MI was calculated only for the modulated responses with a clear peak in the spectrogram at frequency f_1. We regarded a spectrogram value at frequency f_1 as a peak when it exceeded the mean amplitude along all of the frequencies in the spectrogram by at least one standard deviation (SD). We applied the procedure of finding peaks to spectrograms averaged over 12 responses to a stimulus with given parameters $MI = f_1/f_0$ (see Fig. 1).

Results

The activities of 101 visually responsive neurons were recorded in the dorsolateral aspect of the CN in response to drifting sinusoidally modulated gratings. The spectral spatiotemporal visual responses and filter properties of 89 neurons were analyzed in detail. As with earlier findings, our subjective estimation of the extent of the visual receptive fields by recording the neuronal responses to the movements of a light spot generated by a hand-held lamp demonstrated that the visual receptive fields were extremely large: they covered a major part of the contralateral hemifield and extended deep into the ipsilateral hemifield, yielding a receptive field that overlapped almost totally with the visual field of the contralateral eye (Pouderoux & Freton, 1979; Nagy *et al*., 2003b, 2005). For technical reasons and in order to obtain data that could be compared with the findings of our previous studies in the lateral–medial suprageniculate nuclei complex (LM-Sg) of the posterior thalamus (Paróczy *et al*., 2006), the superior colliculus (SC; Waleszczyk *et al*., 2007) and the cortex along the sulcus ectosylvius anterior (AES cortex; Nagy *et al*., 2003a), we consistently centered the stimulation monitor on the area centralis and stimulated a large central part (with a diameter of 30°) of the receptive fields. As the CN visual receptive fields are homogeneous in the sense that the

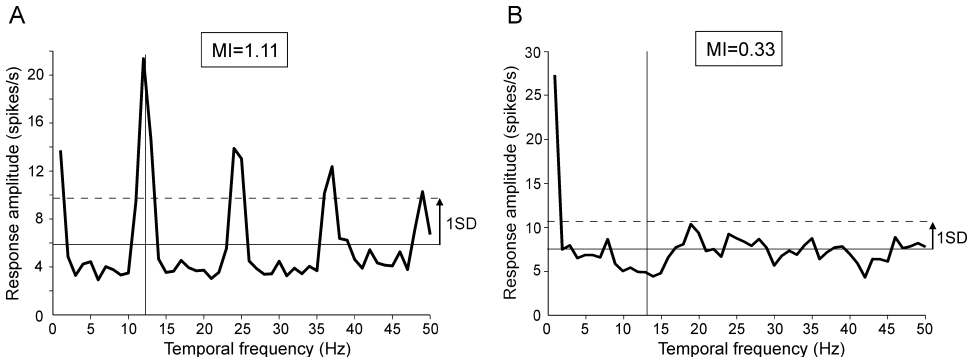

FIG. 1. Determination of the temporal frequency modulation of CN neuron responses (see Materials and methods). Averaged (from 12 trials) spectrograms calculated for neurons responding with modulated (A) or unmodulated (B) activity. The modulation indices are presented in boxes above the spectrograms. The solid horizontal line denotes the mean amplitude of the spectrogram, and the dashed line is one standard deviation (1SD) above the mean. The vertical line indicates the temporal frequency of the stimulus. When the response amplitude in the averaged spectrogram at the fundamental temporal frequency of the stimulus (f_1) exceeded the mean amplitude of the spectrogram by >1SD, the response was classified as modulated.

site of the stimulation within the receptive field has no effect on the velocity, direction or stimulus size preference of a single cell – only the magnitude of the responses can be modulated – (Nagy *et al*., 2003b) stimulation of this large central part of the receptive fields may faithfully describe the spatio-temporal characteristics of the CN.

The mean spontaneous activity of the CN neurons was 9 spikes/s ($n = 101$; SD ±7.4 spikes/s; range 0–32 spikes/s). The CN neurons responded to the drifting gratings with a modulated or unmodulated increase in their discharge rate, although the activities of certain neurons were suppressed for some spatiotemporal frequency combinations and/or directions of the moving gratings.

The responses of 64 (72%) of the 89 CN cells were considered to be modulated by the gratings (see Methods), with clear peaks in the spectrograms at the fundamental frequency f_1 derived from the Fourier transforms of the PSTHs (Fig. 1). *MI* was calculated for the maximal responses (to the optimal stimulus) of each neuron that displayed a modulated response. The mean *MI* was 1.12 ($n = 64$, SD = 0.79, range 0.38–5.1). Twenty-eight CN cells were strongly modulated, with *MI* > 1.0.

Direction selectivity and direction tuning function of the caudate neurons

The direction sensitivity and tuning functions of the CN neurons were determined on the basis of their responses to drifting sinusoidal gratings moving in eight different directions (four different axes of movement). The direction sensitivity of the cells was characterized by using a *DI* (Dreher *et al*., 1993). A majority of the CN neurons (63/101, 62%) exhibited a *DI* of < 50%, and these units were therefore classified as non-direction-sensitive cells. However, 26 of the 101 CN neurons (26%) had *DI* > 70% and were classified accordingly as direction-selectives, while 12 CN neurons (12%) had *DI*s between 50 and 70% and were direction-sensitive (Fig. 2A). The direction tuning of the direction-sensitive and direction-selective CN neurons was characterized by using the direction tuning width, which was defined as the range of directions over which the magnitude of the responses was at least half of the maximal repsonse. The average direction tuning width was 93° ($n = 38$; SD ±51°, range 19–233°, Fig. 2B). The distribution of the direction of the drifting grating that induced the maximal response of the single neurons is presented in Fig. 2C. The direction varied considerably in the cells recorded, but given the moderate number of direction-selective and sensitive cells, it is premature to draw conclusions about the possible rule of distribution in direction preference (Fig. 2C).

Spatial frequency tuning of the CN neurons

The spatial frequency tuning function of the CN neurons was determined on the basis of their responses to drifting sinusoidal gratings moving in the optimal direction with optimal temporal

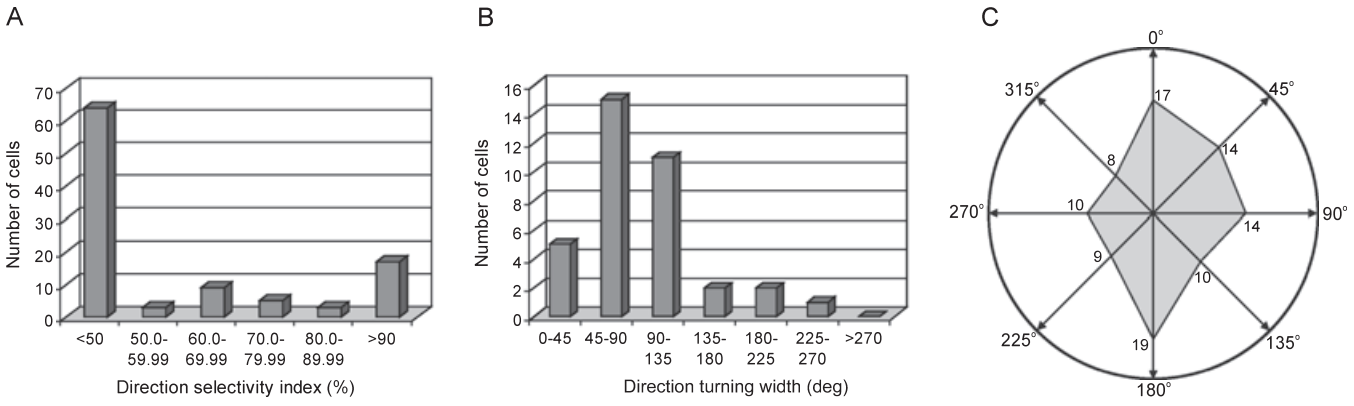

FIG. 2. Direction sensitivity and tuning function of the CN neurons. (A) Distribution of the direction selectivity indices. It should be noted that most of the CN neurons were not direction-sensitive, with *DI*s of < 50%. (B) Direction tuning widths of the direction-sensitive and selective CN units. (C) Distribution of drifting grating directions (indicated by the arrows) that elicited the maximal response amplitude.

frequency. Figure 3A demonstrates the responses of a CN cell to different spatial frequencies. Similarly to this neuron, all of the investigated CN neurons displayed strong responses to very low spatial frequencies. The mean optimal spatial frequency of the CN neurons was 0.05 c/° ($n = 89$, SD ± 0.03 c/°, range 0.025–0.18 c/°; Fig. 4A). The mean optimal spatial frequency may well be overestimated as for 42 neurons the optimal spatial frequency was the lowest (0.025 c/°) tested. The spatial high-frequency cut-off was defined as the frequency at which the net response (after subtraction of the spontaneous activity) of the cell fell to one-tenth of the maximum (Saul & Humphrey, 1990; Waleszczyk *et al*., 2007). This was regarded as a measure of the spatial resolution. The spatial resolution could be calculated for 42 CN units. In this CN neuronal population, the spatial high-frequency cut-off was consistently very low, with a mean of 0.1 c/° ($n = 42$, SD ± 0.05 c/°, range 0.039–0.20 c/°). In contrast to this finding, the responses of the remaining 47 CN neurons were slightly higher than one-tenth of the maximum at the highest spatial frequency tested (Fig. 4B); the spatial resolution for these cells was therefore > 0.4 c/°.

More than half of the investigated CN neurons (55/89, 62%) displayed spatial low-pass tuning characteristics under the present stimulating conditions, with no attenuation of the response for the lowest spatial frequencies (Fig. 5A). Fifteen units (17%) exhibited band-pass spatial frequency tuning (Fig. 5B). The spatial bandwidths measured at half-height of the spatial frequency-tuning curve of the 15 band-pass CN units were analysed (Fig. 4C). The CN units were narrowly tuned to spatial frequencies, and accordingly can serve as good spatial filters. The mean spatial bandwidth of the band-pass-tuned CN neurons was 1.31 octaves ($n = 15$, SD ± 0.76 octaves, range 0.37–3.0 octaves).

Temporal frequency tuning of the CN cells

Sinusoidal gratings at the optimal spatial frequency moving in the optimal direction of each unit were applied to evaluate the temporal frequency tuning of the CN neurons. Similar to the neuron whose responses are demonstrated in Fig. 3B, all of the investigated CN units responded optimally to high temporal frequencies. The mean optimal

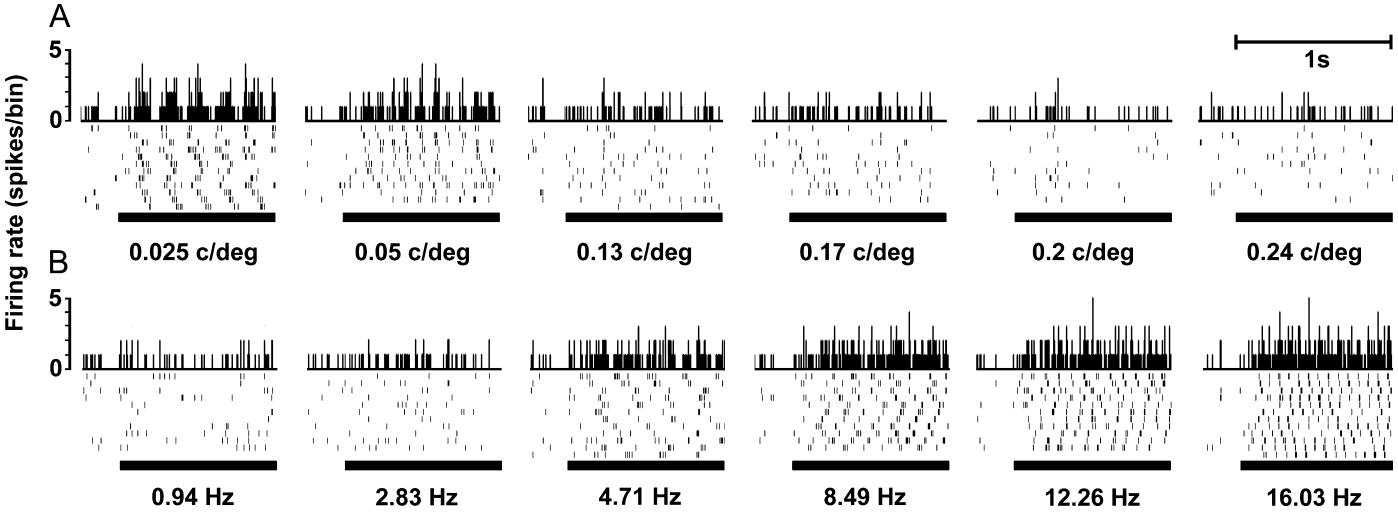

FIG. 3. PSTHs (bin width 10 ms) and raster plots of a temporal frequency-modulated CN cell responding to drifting gratings with different spatial and temporal frequencies. The ordinate denotes the discharge rate (spikes per bin). The thick black lines under the PSTHs indicate the duration of the stimulus movement for 1000 ms (peristimulus time). Corresponding spatial or temporal frequencies of the sinusoidally modulated drifting gratings are shown under the PSTHs. (A) Responses of a CN neuron to six different spatial frequencies (temporal frequency was constant at 5.66 Hz). (B) Responses of the same CN neuron to six different temporal frequencies (spatial frequency was constant at 0.025 c/°).

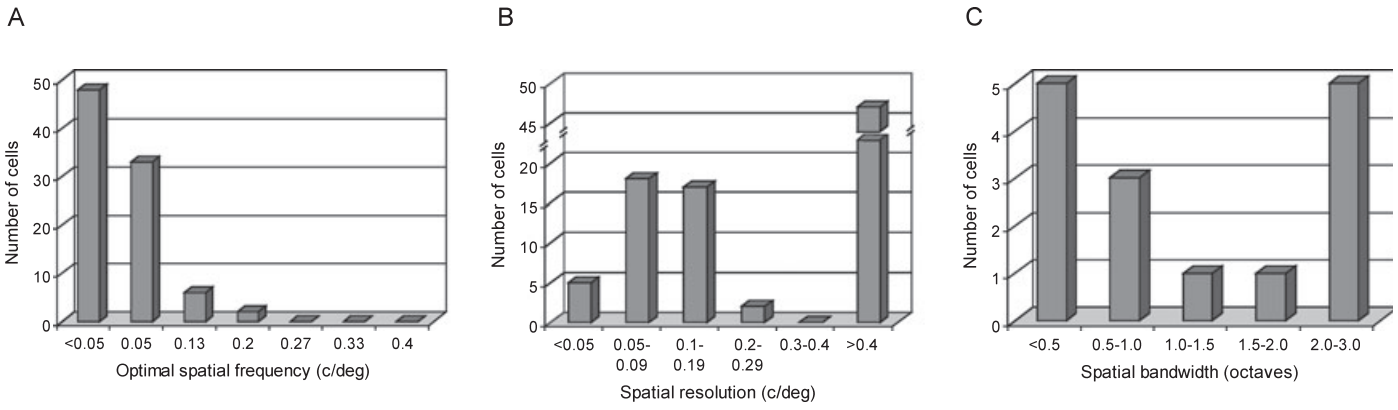

FIG. 4. Visual spatial frequency properties of the CN neurons. (A) Distribution of the optimal spatial frequencies, estimated from the spatial frequency tuning functions. All cells responded optimally to extremely low spatial frequencies. (B) Distribution of the spatial resolutions. (C) Distribution of the spatial bandwidths (full-width at half-height).

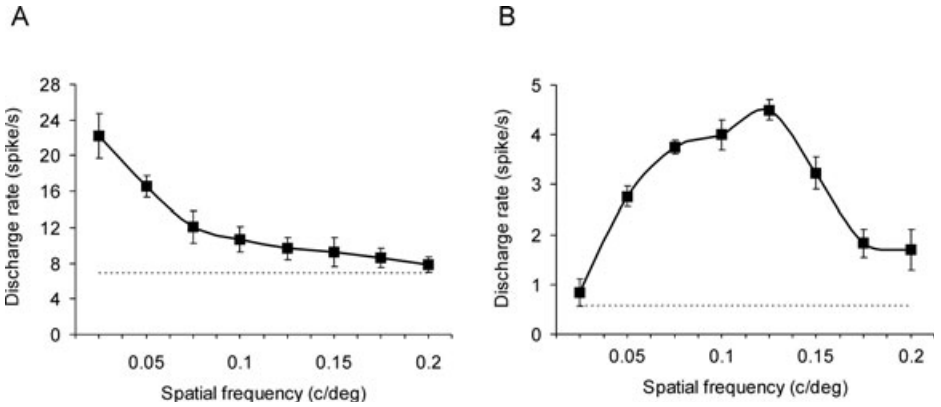

FIG. 5. Examples of spatial frequency tuning functions of the CN neurons. (A) Spatial frequency tuning curve of a spatial low-pass unit. (B) Spatial frequency tuning curve of a band-pass CN neuron. The tuning curves were fitted by using the cubic-spline technique. Each point (square symbol) corresponds to the mean firing rate (f_0 values are presented) during a 1-s grating movement (averaged over 12 stimulus repetitions) for a particular spatial frequency. Each error bar corresponds to the standard error of the mean. The dashed lines indicate the level of spontaneous activity.

temporal frequency of the CN neurons was high: 10.6 Hz ($n = 89$, SD ±4.8 Hz, range 4.6–27.6 Hz; Fig. 6A). The temporal high-frequency cut-off of the CN units was also very high. The mean temporal resolution could be calculated for 31 CN neurons: it was 20.6 Hz ($n = 31$, SD ± 5.6 Hz, range 6.3–34.0 Hz; Fig. 6B). The remaining 58 CN units still showed at least a slight response (higher than one-tenth of the maximal response) for the highest temporal frequency tested.

Fifty-five of the 89 neurons (62%) were classified as temporal band-pass cells (Fig. 7A). The band-pass CN neurons were narrowly tuned to temporal frequencies with a mean temporal bandwidth of 1.38 octaves ($n = 55$, SD ± 1.0 octave, range 0.09–5.36 octaves; Fig. 6C). Fourteen CN neurons (16%) exhibited double temporal frequency tuning with two clear optimal frequencies in the higher temporal frequency domain (Fig. 7B). Six CN units (7%) elicited temporal high-pass tuning (Fig. 7C) and another three (3%) were temporal broad-band neurons. None of the CN units exhibited low-pass temporal frequency tuning.

Discussion

Earlier electrophysiological studies described the responsivity of the CN visual neurons merely to simple geometric forms, i.e. moving spots and bars (Hikosaka *et al*., 1989; Nagy *et al*., 2003b), and were therefore essentially inappropriate to define their responsivity to extended visual stimuli. The present study is the first spectral, spatiotemporal analysis of visual cells in the CN that employs a wide range of spatial and temporal frequencies and describes the particular spectral spatiotemporal filter properties of the CN visual neurons.

Our approach allows a direct comparison of the dynamic properties of the CN with those in other areas of the brain. Table 1 lists the quantitative spatial and temporal visual properties of the subcortical and cortical visual regions investigated to date in the feline brain. The CN cells clearly preferred drifting gratings with extremely low spatial frequencies: the mean optimal spatial frequency of the CN cells was 0.05 c/°. This is a much lower value than those of the X and Y cells of the lateral geniculate nucleus (LGN; Saul & Humphrey, 1990; Humphrey & Murthy, 1999), the lateral posterior–pulvinar complex (LP-Pul) of the thalamus (Casanova *et al*., 1989), and almost all striate and extrastriate visual cortical areas (Movshon *et al*., 1978b; Zumbroich & Blakemore, 1987; Tardif *et al*., 1996, 1997; Morley & Vickery, 1997; Bergeron *et al*., 1998; Nagy *et al*., 2003a), but comparable with those of the SC, the W cells of the LGN and the LM-Sg (Pinter & Harris, 1981; Saul & Humphrey, 1990; Paróczy *et al*., 2006; Waleszczyk *et al*., 2007; Humphrey & Murthy, 1999 Mimeault *et al*., 2004).

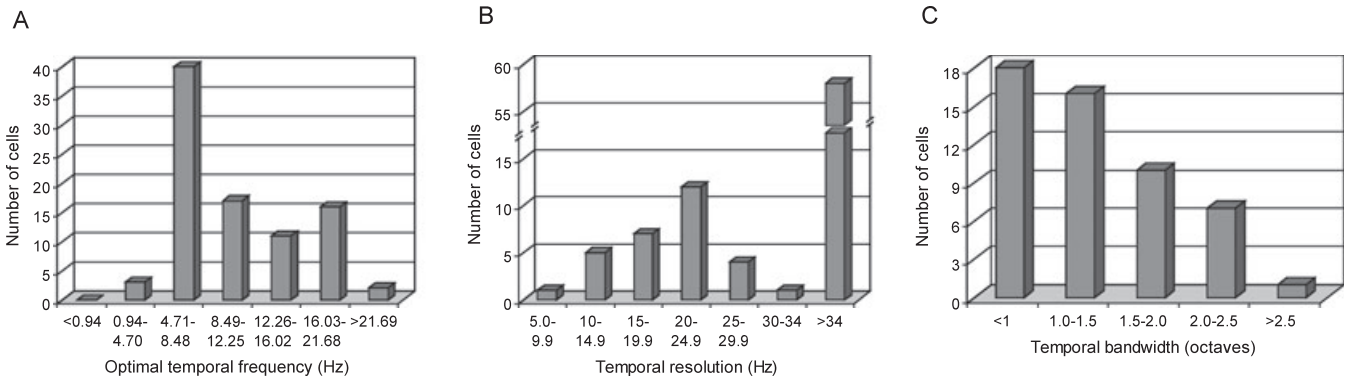

FIG. 6. Visual temporal frequency properties of the CN neurons. (A) Distribution of the optimal temporal frequencies of the cells, estimated from the temporal frequency tuning functions. The CN cells responded optimally to high temporal frequencies. (B) Distribution of the temporal resolution. The CN units consistently had a very high temporal high-frequency cut-off. (C) Distribution of the temporal bandwidths (full-width at half-height). A majority of the cells displayed a relatively narrow temporal tuning.

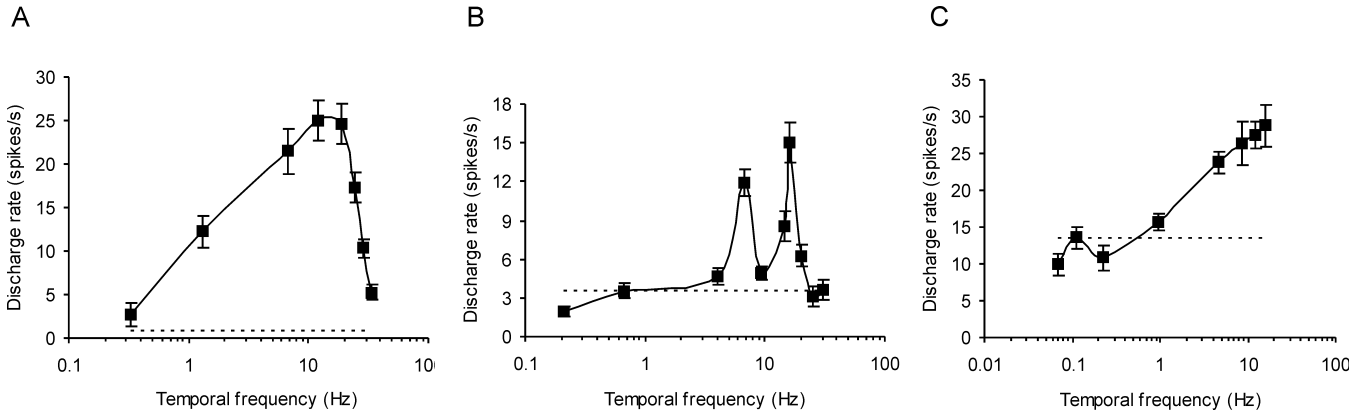

FIG. 7. Examples of temporal frequency tuning functions in the CN. (A) Temporal tuning curve of a band-pass neuron. (B) Tuning curve of a neuron tuned to two temporal frequencies. (C) Tuning curve of a temporal high-pass CN neuron. The tuning curves were fitted by using the cubic-spline technique. The conventions are the same as in Fig. 5.

TABLE 1. Quantitative spatial and temporal visual properties of cortical and subcortical structures in the feline brain

	Optimal spatial frequency (c/°)	Spatial bandwidth (octaves)	Optimal temporal frequency (Hz)	Temporal bandwidth (octaves)
CN	0.05	1.31	10.6	1.38
LM-Sg	0.05	1.07	8.53	1.66
SC	0.10	1.84	6.84	2.38
Lp-Pul	∼0.20	2.20	∼5.00	2.32
LGN X cells	0.85	–	2.50	–
LGN Y cells	0.14	–	5.20	–
LGN W cells	0.07	–	2.70	–
A17	0.90	1.50	2.90	1.70
A18	0.22	1.49	3.20	1.50
A19	0.17	1.90	3.00	2.90
A21a	0.27†, 0.36*	1.60*, 1.79†	3.25†, 7.00*	1.92†, 2.90*
A21b	0.08	2.20	3.20	3.30
PMLS	0.16	2.20	5.00	2.00
AES cortex	0.20	1.40	6.30	1.10

References: *Tardif *et al.* (1996), †Morley & Vickery (1997).

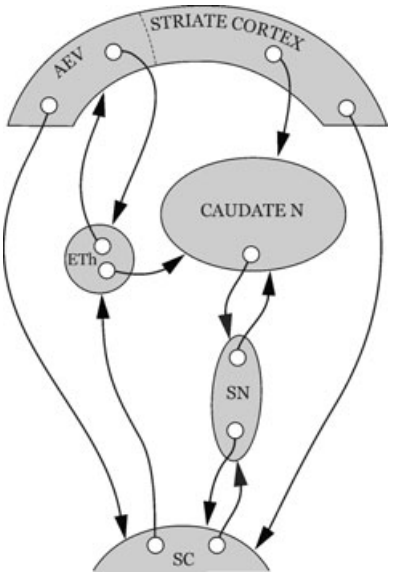

FIG. 8. Visual afferentation of the CN. Black arrows demonstrate the potential interactions between the tectal extrageniculate visual pathway and the CN, and the connection between the striate cortex and the CN. Abbreviations: AEV, anterior ectosylvian visual area; Eth, extrageniculate visual thalamus; SC, superior colliculus; SN, substantia nigra.

A majority of the CN units exhibited low-pass spatial tuning characteristics, although spatial band-pass and broad-band cells were also recorded. Low-pass cells are similarly common in the SC (Pinter & Harris, 1981; Mimeault *et al.*, 2004; Waleszczyk *et al.*, 2007), the posteromedial lateral suprasylvian area (PMLS; Zumbroich & Blakemore, 1987), the anteromedial lateral suprasylvian area (AMLS; Ouellette *et al.*, 2004), the AES cortex (Nagy *et al.*, 2003a) and the LM-Sg of the posterior thalamus (Paróczy *et al.*, 2006). Nevertheless, some low-pass tuned cells have also been observed in cortical areas 17 (Ikeda & Wright, 1975), 18 (Movshon *et al.*, 1978b), 19 (Bergeron *et al.*, 1998), 21a (Morley & Vickery, 1997; Tardif *et al.*, 2000) and 21b (Tardif *et al.*, 2000), the LP-Pul and the LGN of the thalamus (see Saul & Humphrey, 1990 – for X and Y cells; Humphrey & Murthy, 1999 – for W cells) and the W cells of the retina (Rowe & Cox, 1993).

The band-pass CN neurons are narrowly tuned to spatial frequencies with a mean spatial tuning width of 1.31 octaves. This might indicate that the CN cells could act as spatial filters. The spatial tuning width of the band-pass CN neurons is comparable not only with those of the LM-Sg (Paróczy *et al.*, 2006) and the AES cortex (Nagy *et al.*, 2003a), but also with that of the striate visual cortex (Movshon *et al.*, 1978b), but smaller than those of the other visual regions of the feline brain (Tanaka *et al.*, 1987; Zumbroich & Blakemore, 1987; Bergeron *et al.*, 1998; Tardif *et al.*, 2000; Ouellette *et al.*, 2004; Waleszczyk *et al.*, 2007).

All of the investigated CN neurons responded optimally to temporal frequencies >4 Hz. The mean optimal temporal frequency found for the CN cells in this study was 10.6 Hz. This is the highest mean optimal temporal frequency reported for any part of the feline visual cortical or subcortical regions to date. It is slightly higher than those of the SC (Waleszczyk *et al.*, 2007) and the brain regions that receive a tectal source of visual information, and participate in motion analysis, i.e. the LM-Sg (Paróczy *et al.*, 2006), the LP-Pul (Casanova *et al.*, 1989; Merabet *et al.*, 1998), the AES cortex (Nagy *et al.*, 2003a) and the lateral suprasylvian areas (LS; Morrone *et al.* 1986; Zumbroich & Blakemore, 1987; Ouellette *et al.*, 2004), but much higher than those of areas 17 (Saul & Humphrey, 1992; Casanova, 1993), 18 (Saul &

Humphrey, 1992), 19 (Bergeron *et al*., 1998), 21a (Morley & Vickery, 1997) and 21b (Tardif *et al*., 2000), and the X and W cells of the LGN.

The temporal frequency tuning functions of the cells in the CN, similarly to those in the AES cortex (Nagy *et al*., 2003a) and the LM-Sg (Paróczy *et al*., 2006), are mainly band-pass and rarely high-pass. The band-pass CN units displayed narrow temporal frequency tuning at a mean temporal bandwidth of 1.38 octaves. This is comparable with the temporal tuning widths for the LS areas (Morrone *et al*., 1986), the AES cortex (Nagy *et al*., 2003a), areas 17 and 18 (Movshon *et al*., 1978b), and the LM-Sg (Paróczy *et al*., 2006), but much lower than those of the LP-Pul (Casanova *et al*., 1989), and areas 19 (Bergeron *et al*., 1998), 21a (Tardif *et al*., 1996) and 21b (Tardif *et al*., 2000).

There is some degree of uncertainty concerning the pathways conveying sensory information to the basal ganglia. Earlier morphological findings in cats and rabbits stressed the predominant role of the geniculostriate pathway that conveys visual information toward the CN (Webster, 1965; Hollander *et al*., 1979). However, recent morphological and physiological studies support the suggestion that the extrageniculate ascending tectofugal pathways project to the CN in reptiles, birds and mammals (Fig. 8). The dorsolateral, visual part of the CN in the cat can receive its visual afferentation from the LM-Sg of the posterior thalamus, which is connected to the AES cortex with thalamo-cortico-thalamic loops (Harting *et al*., 2001a,b; McHaffie *et al*., 2001; Nagy *et al*., 2003b, 2005; Eördegh *et al*., 2005; Guirado *et al*., 2005). The spatiotemporal visual properties of the CN neurons are extremely similar to those of the subset SC, LM-Sg and the AES cortex (Nagy *et al*., 2003a; Paróczy *et al*., 2006; Waleszczyk *et al*., 2007), with their preference for very low spatial and very high temporal frequencies and narrow spatial and temporal tuning characteristics. It must be mentioned here that areas 17 and 18 have spatial and temporal tuning widths slightly larger, although still comparable (Movshon *et al*., 1978b) with those of the CN. However, this is as far as the similarity goes between the spectral spatiotemporal properties of the CN and areas 17 and 18. Spatial low-pass units are rare in areas 17 and 18, but, similarly to the CN, most common in the extrageniculate subcortical and extrastriate cortical regions (Pinter & Harris, 1981; Casanova *et al*., 1989; Nagy *et al*., 2003a; Paróczy *et al*., 2006; Waleszczyk *et al*., 2007). Further, the optimal spatial and temporal frequency preferences of the CN units are considerably different from those in areas 17 and 18 (Movshon *et al*., 1978b). This suggests that the CN neurons receive strong Y or W signals, probably from the SC, via the LM-Sg of the thalamus and also from the AES cortex (Benedek *et al*., 1996; Nagy *et al*., 2003a, 2005; Eördegh *et al*., 2005; Paróczy *et al*., 2006), and tends to discount high spatial and low temporal frequency X input from area 17 (Movshon *et al*., 1978b).

It is an interesting phenomenon that the drifting gratings strongly modulated the responses of a majority of the CN neurons. While the SC and LM-Sg neurons responded to drifting gratings with a weakly modulated or unmodulated increase in activity (Paróczy *et al*., 2006; Waleszczyk *et al*., 2007), the AES cortex, which possesses strong temporal frequency-modulated discharges (Hicks *et al*., 1988), may be the origin of the modulation in the CN.

The CN neurons are good candidates for tasks involved in the perception of motion and probably in the perception of changes in the visual environment during self-motion (Morrone *et al*., 1986; Brosseau-Lachaine *et al*., 2001), with their extremely large receptive fields (Nagy *et al*., 2003b), their preferences for low spatial frequencies, and their fine spatial and temporal tuning. It has been reported in human psycho-physics investigations that all motion detectors are apparently finely tuned to temporal and spatial frequencies (Anderson & Burr, 1985; Burr & Ross, 1986; Burr *et al*., 1986). The narrow tuning of the CN neurons may contribute to velocity detection and the analysis of the object in motion. These properties enable the CN to play important roles in the recording of movements of the visual environment relative to the body, and in helping its participation in the adjustment of motor behavior to environmental challenges. The fact that the visual properties of the CN neurons closely resemble those described in the extrageniculate tecto-thalamo-cortical visual system supports the notion that the CN may receive its main visual input from interactions among these structures.

Acknowledgements

We thank Ágnes Farkas, Péter Gombkötõ and Andrea Petõ for their help with data collection, Gabriella Dósai, Kálmán Hermann and Joanna Smyda for their valuable technical assistance, and Péter Liszli for computer programming. The work was supported by grants OTKA/Hungary F048396, OTKA/Hungary T42610 and Polish State Committee for Scientific Research 3P04C08222. A.N. is a János Bolyai Research Fellow of the Hungarian Academy.

Abbreviations

AES, anterior ectosylvian sulcus; AMLS, anteromedial lateral suprasylvian area; CN, caudate nucleus; *DI*, direction selectivity index; LGN, lateral geniculate nucleus; LM-Sg, lateral–medial suprageniculate nucleus; LP-Pul, lateral posterior-pulvinar complex; LS, lateral suprasylvian; *MI*, modulation index; PMLS, posteromedial lateral suprasylvian area; PSTH, peristimulus time histogram; SC, superior colliculus.

References

Anderson, S.J. & Burr, D.C. (1985) Spatial and temporal selectivity of the human motion detection system. *Vision Res.*, **25**, 1147–1154.

Barneoud, P., Descombris, E., Aubin, N. & Abrous, D.N. (2000) Evaluation of simple and complex sensorimotor behaviours in rats with a partial lesion of the dopaminergic nigrostriatal system. *Eur. J. Neurosci.*, **12**, 322–336.

Benedek, G., Fischer-Szatmari, L., Kovacs, G., Perenyi, J. & Katoh, Y.Y. (1996) Visual, somatosensory and auditory modality properties along the feline suprageniculate-anterior ectosylvian sulcus/insular pathway. *Prog. Brain Res.*, **112**, 325–334.

Bergeron, A., Tardif, E., Lepore, F. & Guillemot, J.P. (1998) Spatial and temporal matching of receptive field properties of binocular cells in area 19 of the cat. *Neuroscience*, **86**, 121–134.

Bishop, P.O., Kozak, W. & Vakkur, G.J. (1962) Some quantitative aspects of the cats' eye: axis and plane of reference, visual field coordinates and optics. *J. Physiol. (Lond.)*, **163**, 466–502.

Brosseau-Lachaine, O., Faubert, J. & Casanova, C. (2001) Functional subregions for optic flow processing in the posteromedial lateral suprasylvian cortex of the cat. *Cereb. Cortex*, **11**, 989–1001.

Brown, V.J., Desimone, R. & Mishkin, M. (1995) Responses of cells in the tail of the caudate nucleus during visual discrimination learning. *J. Neurophysiol.*, **74**, 1083–1094.

Burr, D.C. & Ross, J. (1986) Visual processing of motion. *Trends Neurosci.*, **9**, 304–307.

Burr, D.C., Ross, J. & Morrone, M. (1986) Seeing objects in motion. *Proc. Roy. Soc. Lond. B.*, **227**, 249–265.

Casanova, C. (1993) Response properties of neurons in area 17 projecting to the striate-recipient zone of the cat's lateralis posterior-pulvinar complex: comparison with cortico-tectal cells. *Exp. Brain Res.*, **96**, 247–259.

Casanova, C., Freeman, R.D. & Nordmann, J.P. (1989) Monocular and binocular response properties of cells in the striate-recipient zone of the cat's lateral posterior-pulvinar complex. *J. Neurophysiol.*, **62**, 544–557.

De Valois, K.K., De Valois, R.L. & Yund, E.W. (1979) Responses of striate cortex cells to grating and checkerboard patterns. *J. Physiol.*, **291**, 483–505.

Dreher, B., Michalski, A., Ho, R.H., Lee, C.W. & Burke, W. (1993) Processing of form and motion in area 21a of cat visual cortex. *Vis. Neurosci.*, **10**, 93–115.

Enroth-Cugell, C. & Robson, J.G. (1966) The contrast sensitivity of retinal ganglion cells of the cat. *J. Physiol.*, **187**, 517–552.

Eördegh, G., Nagy, A., Berényi, A. & Benedek, G. (2005) Processing of spatial visual information along the pathway between the suprageniculate nucleus and the anterior ectosylvian cortex. *Brain Res. Bull.*, **67**, 281–289.

Guirado, S., Real, M.A. & Davila, J.C. (2005) The ascending tectofugal visual system in amniotes: new insights. *Brain Res. Bull.*, **66**, 290–296.

Harting, J.K., Updyke, B.V. & Van Lieshout, D.P. (2001a) Striatal projections from the cat visual thalamus. *Eur. J. Neurosci.*, **14**, 893–896.

Harting, J.K., Updyke, B.V. & Van Lieshout, D.P. (2001b) The visual-oculomotor striatum of the cat: functional relationship to the superior colliculus. *Exp. Brain Res.*, **136**, 138–142.

Hicks, T.P., Benedek, G. & Thurlow, G.A. (1988) Organization and properties of neurons in a visual area within the insular cortex of the cat. *J. Neurophysiol.*, **60**, 397–421.

Hikosaka, O., Sakamoto, M. & Usui, S. (1989) Functional properties of monkey caudate neurons. II. Visual and auditory responses. *J. Neurophysiol.*, **61**, 799–813.

Hikosaka, O., Takikawa, Y. & Kawagoe, R. (2000) Role of the basal ganglia in the control of purposive saccadic eye movements. *Physiol. Rev.*, **80**, 953–978.

Hollander, H., Tietze, J. & Distel, H. (1979) An autoradiographic study of the subcortical projections of the rabbit striate cortex in the adult and during postnatal development. *J. Comp. Neurol.*, **184**, 783–794.

Humphrey, A.L. & Murthy, A. (1999) Cell types and response timings in the medial interlaminar nucleus and C-layers of the cat lateral geniculate nucleus. *Vis. Neurosci.*, **16**, 513–525.

Ikeda, H. & Wright, M.J. (1975) Spatial and temporal properties of 'sustained' and 'transient' neurones in area 17 of the cat's visual cortex. *J. Physiol. (Lond.)*, **22**, 363–383.

Kolomiets, B. (1993) A possible visual pathway to the cat caudate nucleus involving the pulvinar. *Exp. Brain Res.*, **97**, 317–324.

Lynd-Balta, E. & Haber, S.N. (1994) The organization of midbrain projections to the striatum in the primate: sensorimotor-related striatum versus ventral striatum. *Neuroscience*, **59**, 625–640.

McHaffie, J.G., Thomson, C.M. & Stein, B.E. (2001) Corticotectal and corticostriatal projections from the frontal eye fields of the cat: an anatomical examination using WGA-HRP. *Somatosens. Mot. Res.*, **18**, 117–130.

Merabet, L., Desautels, A., Minville, K. & Casanova, C. (1998) Motion integration in a thalamic visual nucleus. *Nature*, **396**, 265–268.

Mimeault, D., Paquet, V., Molotchnikoff, S., Lepore, F. & Guillemot, J.P. (2004) Disparity sensitivity in the superior colliculus of the cat. *Brain Res.*, **1010**, 87–94.

Morley, J.W. & Vickery, R.M. (1997) Spatial and temporal frequency selectivity of cells in area 21a of the cat. *J. Physiol. (Lond.)*, **501**, 405–413.

Morrone, M.C., Di Stefano, M. & Burr, D.C. (1986) Spatial and temporal properties of neurons of the lateral suprasylvian cortex of the cat. *J. Neurophysiol.*, **56**, 969–986.

Movshon, J.A., Thompson, I.D. & Tolhurst, D.J. (1978a) Spatial summation in the receptive fields of simple cells in the cat's striate cortex. *J. Physiol. (Lond.)*, **283**, 53–77.

Movshon, J.A., Thompson, I.D. & Tolhurst, D.J. (1978b) Spatial and temporal contrast sensitivity of neurones in areas 17 and 18 of the cat's visual cortex. *J. Physiol. (Lond.)*, **283**, 101–120.

Nagy, A., Eördegh, G. & Benedek, G. (2003a) Spatial and temporal visual properties of single neurons in the feline anterior ectosylvian visual area. *Exp. Brain Res.*, **151**, 108–114.

Nagy, A., Eördegh, G., Norita, M. & Benedek, G. (2003b) Visual receptive field properties of neurons in the feline caudate nucleus. *Eur. J. Neurosci.*, **18**, 449–452.

Nagy, A., Paróczy, Z., Norita, M. & Benedek, G. (2005) Multisensory responses and receptive field properties of neurons in the substantia nigra and in the caudate nucleus. *Eur. J. Neurosci.*, **22**, 419–424.

Ouellette, B.G., Minville, K., Faubert, J. & Casanova, C. (2004) Simple and complex visual motion response properties in the anterior medial bank of the lateral suprasylvian cortex. *Neuroscience*, **123**, 231–345.

Paróczy, Z., Nagy, A., Márkus, Z., Waleszczyk, W.J., Wypych, M. & Benedek, G. (2006) Spatial and temporal visual properties of single neurons in the suprageniculate nucleus of the thalamus. *Neuroscience*, **137**, 1397–1404.

Pettigrew, J.D., Cooper, M.L. & Blasdel, G.G. (1979) Improved use of tapetal reflection for eye-position monitoring. *Invest. Ophthalmol. Vis. Sci.*, **18**, 490–495.

Pinter, R.B. & Harris, L.R. (1981) Temporal and spatial response characteristics of the cat superior colliculus. *Brain Res.*, **207**, 73–94.

Pouderoux, C. & Freton, E. (1979) Patterns of unit responses to visual stimuli in the cat caudate nucleus under chloralose anesthesia. *Neurosci. Lett.*, **11**, 53–58.

Rolls, E.T., Thorpe, S.J. & Maddison, S.P. (1983) Responses of striatal neurons in the behaving monkey. 1. Head of the caudate nucleus. *Behav. Brain Res.*, **7**, 179–210.

Rowe, M.H. & Cox, J.F. (1993) Spatial receptive-field structure of cat retinal W cells. *Vis. Neurosci.*, **10**, 765–779.

Saul, A.B. & Humphrey, A.L. (1990) Spatial and temporal response properties of lagged and nonlagged cells in cat lateral geniculate nucleus. *J. Neurophysiol.*, **64**, 206–224.

Saul, A.B. & Humphrey, A.L. (1992) Temporal-frequency tuning of direction selectivity in cat visual cortex. *Vis. Neurosci.*, **8**, 365–372.

Strecker, E.R., Steinfels, G., Abercrombie, E.D. & Jacobs, B.L. (1985) Caudate unit activity in freely moving cats: effects of phasic auditory and visual stimuli. *Brain Res.*, **329**, 350–353.

Tanaka, K., Ohzawa, I., Ramoa, A.S. & Freeman, R.D. (1987) Receptive field properties of cells in area 19 of the cat. *Exp. Brain Res.*, **65**, 549–558.

Tardif, E., Bergeron, A., Lepore, F. & Guillemot, J.P. (1996) Spatial and temporal frequency tuning and contrast sensitivity of single neurons in area 21a of the cat. *Brain Res.*, **716**, 219–223.

Tardif, E., Lepore, F. & Guillemot, J.P. (2000) Spatial properties and direction selectivity of single neurons in area 21b of the cat. *Neuroscience*, **97**, 625–634.

Tardif, E., Richer, L., Bergeron, A., Lepore, F. & Guillemot, J.P. (1997) Spatial resolution and contrast sensitivity of single neurons in area 19 of split-chiasm cats: a comparison with primary visual cortex. *Eur. J. Neurosci.*, **9**, 1929–1939.

Villeneuve, M.Y. & Casanova, C. (2003) On the use of isoflurane versus halothane in the study of visual response properties of single cells in the primary visual cortex. *J. Neurosci. Methods*, **129**, 19–31.

Waleszczyk, W.J., Nagy, A., Wypych, M., Berényi, A., Paróczy, Z., Eördegh, G., Ghazaryan, A. & Benedek, G. (2007) Spectral receptive field properties of neurons in the feline superior colliculus. *Exp. Brain Res.*, **181**, 87–98.

Webster, K.E. (1965) The cortico-striatal projections in the cat. *J. Anat.*, **99**, 329–337.

Zumbroich, T.J. & Blakemore, C. (1987) Spatial and temporal selectivity in the suprasylvian visual cortex of the cat. *J. Neurosci.*, **7**, 482–500.

Zumbroich, T., Price, D.J. & Blakemore, C. (1988) Development of spatial and temporal selectivity in the suprasylvian visual cortex of the cat. *J. Neurosci.*, **8**, 2713–2728.